Quantifying and engineering probiotic bacterial adhesion to mucus

Zachary J. S. Mays[1], Todd C. Chappell[1], and Nikhil U. Nair[1*]

[1]Department of Chemical and Biological Engineering, Tufts University, Medford, MA, 02155

[*]Correspondence: nikhil.nair@tufts.edu or @nair_lab

KEYWORDS

Lactic acid bacteria; probiotics; microbiome; cell adhesion; mucus; mucoadhesion

ABSTRACT

Mucus in the gastrointestinal (GI) tract is the primary point-of-interaction between humans and their gut microbiota. This not only intimates that mucus ensures protection against endogenous and exogenous opportunists but provision for the human microbiota to reside and flourish. With the emergence of living therapeutics, engineered microbes can deliver and produce increasingly complex medicine, and controlling the mucoadhesive properties of different microbial chassis can dictate dose-response in a patient. Here we present a redesigned, *in vitro*, plate-based assay to measure the mucus adhesion of various probiotics. Cell-mucus interactions were isolated by immobilizing mucus to the plate surface. Binding parameters were derived for each probiotic strain by measuring cell adhesion over a wide range of cell concentrations, providing dose-dependent adhesion metrics. Surface proteins and cell components known to influence mucoadhesion were then heterologously expressed or altered in *Lactococcus lactis* MG1363 and *E. coli* Nissle 1917 to control mucus-binding capacity, avidity, and cooperativity.

INTRODUCTION

As a new era of precision medicine and personalized therapeutics becomes increasingly mainstream, there too is heightened interest in our ability to leverage the human gut microbiota, a complex and rich community of approximately 1000 species of microbes living in the gastrointestinal (GI) tract. Although causality remains uncertain,

recent evidence suggests a strong relationship between many disease states and a perturbed, dysbiotic, gut microbiota (Cho and Blaser, 2012; Shreiner, Kao and Young, 2015). One strategy to restore microbial balance, and the basis of 282 clinical trials in the last decade (US National Library of Medicine, 2018), is to introduce probiotics – microbes shown to confer health benefits. Probiotics have been shown to inhibit or exclude enteric pathogens (Ollech *et al.*, 2016; Shafaghi *et al.*, 2016), modulate or improve mucosal barrier function (Mennigen *et al.*, 2009), reduce inflammatory responses (Gionchetti *et al.*, 2003), ameliorate metabolic or toxin imbalances (Krishnan *et al.*, 2018), maintain intestinal pH, and contribute to neurohumoral signaling (Hyland and Stanton, 2016). Furthermore, engineered probiotics as therapeutic delivery vehicles (Waller *et al.*, 2017; Bober, Beisel and Nair, 2018; Mays and Nair, 2018) are being explored for pathogen eradication (Hwang *et al.*, 2017), vaccines (Rosales-Mendoza, Angulo and Meza, 2016), metabolic disorders, enzyme-replacement therapies (Isabella *et al.*, 2018; West *et al.*, 2019), cancer treatments (Zhang *et al.*, 2012; Chowdhury *et al.*, 2019), and diagnostics (Danino *et al.*, 2015; Riglar *et al.*, 2017).

Somewhat counterintuitively, the stability of a healthy gut microbiota likely arises from its diversity and competitiveness rather than established cooperative metabolic networks (Coyte, Schluter and Foster, 2015). Thus, an argument can be made that when developing probiotic therapeutics, one design focus should be to enhance factors conferring competitive opportunity (of course, while safeguarding against overgrowth). This dichotomy is further exemplified by the fact that lactic acid bacteria (LAB), which encompass the majority of common probiotics studied for disease amelioration, make up less than 1% of the human microbiota (Douillard and de Vos, 2014). Furthermore, orally-administered probiotics are rarely detected past a week after ingestion, and persistence is highly strain- and patient-specific (Derrien and van Hylckama Vlieg, 2015), making dose-response relationships unreliable (Ouwehand, 2017). From an engineering perspective, directing a microbe toward a synthetic application inherently places a burden that conciliates competitive advantage against its natural counterpart in the body; essentially, current strategies cannot compete with the autochthonous members of the microbiota.

The most prominent point-of-interaction between microbes and humans is at mucus membranes, revealing mucus adhesion as a prime target for controlling probiotic occupancy. Indeed, the cell-surface structures of com-

mensal bacteria are hypothesized to have coevolved in the presence of mucus glycans, creating preferential mucoadhesive mechanisms (Boekhorst *et al.*, 2006). Additionally, the extracellular polysaccharides (EPS) secreted for LAB biofilm formation can influence colonization through mucus associations (Lebeer *et al.*, 2009; Salas-Jara *et al.*, 2016), while pathogenic biofilm formation is impeded by LAB extracellular polysaccharides and mucus itself (Caldara *et al.*, 2012). Mucin has also been observed to increase surface-protease expression in LAB, suggesting the utilization of mucus as a nutrient source (Wickström *et al.*, 2013). Despite these interactions and the mucus matrix of the GI tract providing a topography for microbes to find spatial niches, orally-administered natural probiotics and engineered microbial therapeutics do not currently provide any means of controlling biogeographical targeting, residence time, or an ability to colonize the gut. The ability to accurately measure and engineer mucus adhesion could address these limitations and provide a new avenue to increase efficacy of natural and engineered probiotic therapies.

Methodologies to quantify bacterial adhesion to mucus have been adapted from traditional cell adhesion assays and inherit similar advantages and disadvantages (Mackie *et al.*, 2017). The general procedure behind these adhesion assays is to quantify the fraction of residual bacteria bound to mucus-functionalized surfaces after washes (Khalili and Ahmad, 2015). Surfaces are often modified by incubating with mucus or by culturing gut epithelial cell/organ tissue. However, recent studies showed that bacteria adhere to polystyrene, the support of mucus functionalization, as well or better than mucin- or cell culture-coated microplate wells (Laparra and Sanz, 2009). Additionally, there are several examples of bacterial strains showing different adhesion characteristics depending on the mucus source (Li *et al.*, 2008; MacKenzie *et al.*, 2010; Le *et al.*, 2013), and different mucus compositional profiles can be observed in co-culture models simply by differentiating the HT29 cell line with either methotrexate (MTX) or 5-fluorouracil (FU) (Leteurtre *et al.*, 2004). The question arises then, whether these adhesion data are the result of the mucus composition affecting cell-cell associations, cell-mucus associations, or mucus-plastic associations. Measuring more holistic binding parameters when quantifying mucus adhesion would allow for better comparability across conditions.

72 In order to address these disconnects, we report an improved *in vitro* method for quantifying bacterial adhe-
73 sion to mucus. Rather than relying on natural nonspecific interactions to coat a microplate with mucus, we cova-
74 lently functionalized surfaces with mucus, providing robust and full coverage. Our assay is able to isolate the cell
75 adhesion events associated directly with mucus. We then measure adhesion over a range of cell concentrations to
76 develop strain-specific mucus-binding curves. By more clearly describing mucus adhesion using global quantifiers,
77 we can better compare various binding characteristics related to binding capacity, binding avidity, and
78 cooperativity for common probiotic strains as well as engineered strains. We also demonstrate how the expression
79 of recombinant characterized and putative mucus-binding proteins, or deletion thereof, can be used to alter mu-
80 cus-binding characteristics of probiotics and how these changes are reflected in the binding curves. Such altered
81 mucus-binding has never been engineered previously. Overall, our methods and results provide a novel and ro-
82 bust approach to quantifying bacterial adhesion to mucus and advances design of microbial therapeutics with
83 tunable pharmacological release factors.

84 RESULTS AND DISCUSSION

85 Silanization and EDC-coupling covalently binds mucus to the plate surface

86 A comparison of traditional *in vitro* models used to study bacterial adhesion to the intestinal epithelium re-
87 vealed that differences between bacterial strains binding to mucus are significantly confounded by their ability to
88 strongly stick to the abiotic surface of the microplate (Laparra and Sanz, 2009). To remedy this, we sought to cova-
89 lently link mucus to the plate, providing full mucus coverage and removing cell-plate interactions. To perform this,
90 the microplate surface was silanized with (3-aminopropyl)triethoxysilane (APTES) to provide a surface of available
91 primary amine groups. The most abundant mucin protein in the small intestine is Muc2, which is dominated by
92 sialylated and sulfated glycans, providing freely accessible carboxyl groups (Larsson *et al.*, 2009; Koropatkin, Cam-
93 eron and Martens, 2012). Using the primary amine on the plate and available carboxyl groups of terminal glycans
94 of PIM, porcine intestinal mucus (PIM) was then crosslinked to the silanized microplate using a common *N*-ethyl-
95 *N'*-(3-dimethyl-aminopropyl) carbodiimide and *N*-hydroxysuccinimide (EDC/NHS) reaction mixture (Figure 1).

96 Previous reports indicate that it is possible to immobilize mucus using EDC-coupling, wherein mucus provides
97 primary amine groups for the reaction (Uchida *et al.*, 2004). Because our proposed reaction scheme requires mu-
98 cin to donate carboxyl groups, we wanted to confirm that EDC-coupling was indeed possible with the plate sur-
99 face and that the reaction was not hindered by a self-reaction involving amines within the mucins themselves. To
100 accomplish this, we performed two EDC reactions in tandem. First, between sulfo-cyanine5 amine (cya5) and PIM
101 in which mucus provides carboxyl groups and a subsequent filtration removes any unbound fluorophore. Second,
102 between PIM and the microplate in which vigorous wash steps can separate non-specifically bound mucus from
103 that which is covalently attached to the plate. Fluorescence was observed before and after washing, and the pres-
104 ence of mucus was confirmed by a follow-up Muc2-specific enzyme-linked immunosorbent assay (ELISA) (Figure
105 2a). As shown in Figure 2b, when both EDC-coupling reactions are performed, not only is fluorescence observed
106 initially, suggesting covalent linking to the mucus, but it remains after multiple washes, suggesting the mucus is
107 stably linked to the microplate surface. Absence of the EDC reagent at either stage results in no fluorescence or
108 plate binding, as expected. Similar results were observed from the subsequent Muc2-specific ELISA (Figure 2c).
109 These results confirm the directionality of the EDC-coupling reaction and that mucus was covalently bound to the
110 microtiter plate. Covalently bound mucus provided further opportunities for optimizing the cell adhesion assay,
111 including automated wash steps.

112 Modified microtiter plate assay reveals dependence of cell adhesion on mucus type

113 Bacterial strains isolated from mammalian intestines have been reported to preferentially bind mucus over
114 other general proteins such as bovine serum albumin (BSA) (MacKenzie *et al.*, 2010). Unfortunately, when using
115 the traditional cell adhesion assay to test the mucoadhesive ability of *Lactobacillus reuteri* ATCC PTA-6475 at
116 OD_{600} 0.5, we were not able replicate preferential binding to mucus over BSA (Figure 2d). Only after implementing
117 our newly modified covalent immobilization, did we observe significant differences between binding to polysty-
118 rene plate, BSA, porcine gastric mucus (PGM), and PIM by *L. reuteri* ATCC PTA-6475. Specifically, there was a larger
119 percent of adhered *L. reuteri* ATCC PTA-6475 cells to PIM than the plate, BSA, and PGM (Figure 2d), potentially
120 recapitulating this strain's co-evolution with, and preferential binding to, intestinal niches. It has been previously

121 reported that mucus gel reconstituted from commercially available PGM does not accurately replicate the pH-
122 dependent rheological characteristics of native mucus (Celli *et al.*, 2007) and has an altered structure, likely from
123 industrial processing (Wagner, Wheeler and Ribbeck, 2018). Sialic acid content is an important determinant of the
124 viscosity and elasticity of mucus (Zanin *et al.*, 2016), which may explain the diminished cell adhesion capacity ob-
125 served with PGM (Figure 2d).

126 We obtained similar preferential binding to covalently immobilized PIM at a high cell density (OD_{600} 10.0) of *L.*
127 *reuteri* ATCC PTA-6475 while the traditional assay demonstrated equivalent and non-specific maximum binding
128 capacity of 35% under all conditions (Figure 2d). This was likely observed because the more vigorous washing re-
129 quired at higher cell loadings removes non-covalently attached proteins from the plastic surface. Additionally,
130 while *L. reuteri* ATCC PTA-6475 did not appear to bind any better to PGM than BSA or the plate at the low cell
131 density, the binding capacity significantly increased at the higher cell density, becoming significantly higher than
132 the 35% maximum threshold of the uncoated plate (Figure 2d). It can then be inferred that covalently immobilized
133 mucus enables detection of specific cell-mucus interactions rather than non-specific cell-plastic binding events
134 that dominate with non-covalently functionalized plates. A final important aspect of the new assay is a higher
135 throughput and automated wash procedure, adding consistency between technician operability without sacrific-
136 ing replicate variability.

137 Different probiotics display vastly different mucoadhesive characteristics

138 Cell mucoadhesion is typically reported as a percent or fractional residual bound cells at a single cell concen-
139 tration, often at OD_{600} 0.5 (Jonsson, Ström and Roos, 2001; Roos and Jonsson, 2002; Li *et al.*, 2008; MacKenzie *et*
140 *al.*, 2010; Etzold *et al.*, 2014; Jensen *et al.*, 2014). To assess binding characteristics in greater resolution, we meas-
141 ured adhesion of several probiotic strains and species across a wide range of cell concentrations (OD_{600} 0.01 to
142 100). While there are some previous reports measuring dose-dependent adhesion of probiotics, these were either
143 performed using a Caco2 monolayer (Lee *et al.*, 2000), therein not directly measuring mucus adhesion, or per-
144 formed at very low cell concentrations ($OD_{600} < 0.1$), likely due to the limited dynamic range of the traditional as-
145 say (Mukherjee and Ramesh, 2015). With our more robust immobilized mucus plate, we aimed to develop a more

146 quantitative and descriptive mucoadhesive measurement by expanding the dose range, introducing shear stress in
147 the form of orbital plate shaking, and fitting a sigmoidal curve to the adhesion data to make direct comparisons
148 without the need to normalize between strains. With many cell-mucus interactions determined to be lectin-like
149 recognition of mucus glycans by surface proteins (Tallon *et al.*, 2007; Petrova *et al.*, 2016; Valeriano *et al.*, 2016;
150 Latousakis *et al.*, 2019), a sigmoidal Hill-type shape (Hill, 1910) was chosen with the hypothesis that cell-mucus
151 binding mirrors the energetics of ligand-receptor binding.

152 Using this method, distinct strain-specific differences between the mucoadhesive abilities of common probiot-
153 ics become apparent (Figure 3). This was particularly interesting for *L. reuteri* human isolates. *L. reuteri* ATCC PTA-
154 6475 and *L. reuteri* ATCC PTA-5289, which are nearly identical at the genome level (Walter, Britton and Roos, 2011)
155 clustered in the MLSA (multilocus sequence analysis) lineage II phylogenic group (Oh *et al.*, 2010). Notably, these
156 strains also contain variations of cell and mucus-binding protein A (CmbA) (Jensen *et al.*, 2014) and have been
157 previously reported to have strong adhesion to mucus and intestinal epithelial cells (IEC) (Jensen *et al.*, 2012). In
158 contrast, *L. reuteri* DSM 17938 is from a different phylogenic branch (lineage VI) and has a much lower reported
159 adherence to IECs (Jonsson, Ström and Roos, 2001), which concurs with our observation that it attains a low max-
160 imum adherence capacity (A_{max} = 4.3×10^7 cells/cm^2).

161 *Escherichia coli* Nissle 1917 (EcN) is an extensively studied probiotic sold over-the-counter as Mutaflor® to
162 treat chronic inflammatory and infectious intestinal diseases and is significantly used in the development of mi-
163 crobial therapeutics (Lasaro *et al.*, 2009; Hancock, Dahl and Klemm, 2010; Joeres-Nguyen-Xuan *et al.*, 2010; Maltby
164 *et al.*, 2013; Ou *et al.*, 2016; Scaldaferri *et al.*, 2016; West *et al.*, 2019). Though there are conflicting reports whether
165 EcN can persist in human intestines (Anderson *et al.*, 2003; Hancock, Dahl and Klemm, 2010), it has been shown to
166 colonize the porcine intestine al tract. Surprisingly, therefore, our results inicate a surprisingly poor ability to ad-
167 here to PIM, as determined by this assay (A_{max} 12.9×10^7 cells/cm^2). Like *L. reuteri* DSM 17938, its binding plateaus
168 to its maximum relatively easily (Table 1). It has been suggested that biofilm-like aggregation is necessary for EcN
169 colonization (Kankainen *et al.*, 2009) and that mucoadhesion is influential in initial binding before other competi-
170 tive mechanisms take over. Additionally, compared to pathogenic strains, commensal *E. coli* have more flexibility

171 in their ability to perform metabolic shifts depending on the mono- and disaccharide carbon sources available
172 from mucin glycans (Fabich *et al.*, 2008). This suggests commensal *E. coli*, such as EcN, may utilize mucus by find-
173 ing a nutritional niche rather than adhering as a persistence mechanism.

174 Another commonly used clinical probiotic is *Lactobacillus rhamnosus* GG (ATCC 53103), which has been report-
175 ed to have strong mucoadhesion primarily through SpaCBA pilus-mediated interactions (Nishiyama, Sugiyama
176 and Mukai, 2016). Notably, both EcN and *L. rhamnosus* GG show moderate mucus-binding ability and use moon-
177 lighting proteins with the secondary function of mucus adhesion but have quite different binding characteristics.
178 While the probiotic nature of *Weissella confusa* is in question (Fairfax, Lephart and Salimnia, 2014), it was observed
179 to have a similar binding capacity (A_{max} 45 $\times 10^7$ cells/cm^2) to *L. rhamnosus* GG, which corroborates a report of the-
180 se strains binding strongly to HT29-MTX, a mucus-producing differentiated epithelial cell line (Ayeni *et al.*, 2011).

181 Finally, *Lactococcus lactis* MG1363 is undoubtedly the most well-studied LAB and the basis of centuries of food
182 engineering. Importantly, *L. lactis* MG1363 showed poor binding ability to PIM compared to other probiotic strains
183 (Figure 3g). Despite similar curve parameters to *L. reuteri* DSM 17938, *L. lactis* MG1363 has a higher sigmoidal co-
184 efficient, creating a tighter window of concentrations in which mucus binding is influential compared to other
185 strains.

186 Expression or removal of surface proteins can be used to alter adhesion characteristics

187 There are several surface proteins characterized on LAB that either moonlight or directly mediate
188 mucoadhesion (Jensen *et al.*, 2014). A database search revealed a number of known and putative mucus-
189 associated proteins found on the *L. reuteri* strains being evaluated. Constitutively expressing three of these pro-
190 teins in *L. lactis* MG1363 highly, moderately, and minimally altered the stain mucoadhesion characteristics.

191 Cell and mucus-binding protein (CmbA) has been reported to significantly impact the ability of *L. reuteri* ATCC
192 PTA-6475 to bind to Caco-2 cells and PIM (Boekhorst *et al.*, 2006). The protein also contains a 288 base pair tan-
193 dem repeat region, a characteristic found in surface proteins associated with mucus binding in various LAB (Båth
194 *et al.*, 2005). When expressing CmbA on the surface of *L. lactis* MG1363, the mucus-binding ability of the strain

195 drastically improved, creating a binding curve with similar parameters to that of *L. reuteri* ATCC PTA-6475 (Figure
196 4a and Table 2).

197 Despite the observed poor mucus-binding ability of *L. reuteri* DSM 17938, the cell surface of *L. reuteri* SD2112,
198 the genetically equivalent parental strain, has been characterized with multiple identified putative mucus binding
199 proteins, including Lr0793 and Lr1064 (Aleljung *et al.*, 1994; Roos *et al.*, 1996). The protein Lr0793 is an ATP-
200 binding cassette (ABC)-transporter component of an amino acid transporter, homologous to collagen-binding
201 protein (CnBP) and mucus adhesion promoting protein A (MapA) with 97% sequence identity. These homologs
202 have been described as binding to collagen type I (Rojas, Ascencio and Conway, 2002), gastric mucus (Saraiva *et*
203 *al.*, 2015), and Caco-2 cells (Båth *et al.*, 2005). However, expressing Lr0793 on the surface of *L. lactis* MG1363 only
204 slightly improved maximum adherence capacity to PIM compared to wild-type while OD_{A50} remained unchanged
205 (Figure 4c and Table 2). Similarly, Lr1064 is an ABC-transporter component of a metal ion transporter and member
206 of the LraI family (Jenkinson, 1994). These proteins have been reported to be adhesins of oral streptococci (Båth *et*
207 *al.*, 2005). When expressed on *L. lactis* MG1363, Lr1064 increased the maximum adherence capacity (27.8×10^7
208 cells/cm^2) while keeping the OD_{A50} similar to wild-type, thus moderately improving mucoadhesion (Figure 4b and
209 Table 2). Additionally, when testing the binding ability of *L. lactis* expressing Lr1064 on BSA rather than PIM, there
210 was no observed improved adhesion, reinforcing the observed differences are in fact mucus-specific cell adhesion
211 caused from surface protein expression (Figure S1). These studies demonstrate binding curved of recombinant *L.*
212 *lactis* recapitulates those of the strain from which the mucus binding proteins were sourced.

213 Expression of each mucus-associated protein was confirmed by Western Blot (Figure S2), and surface display
214 was confirmed by flow cytometry (Figure S3) using anti-His-tag antibodies. The pSIP expression vectors have pre-
215 viously shown successful secretion of the reporter nuclease A (NucA) in LAB (Troge *et al.*, 2012). We displayed an
216 inactive mutant ($NucA^{E41Q}$) on *L. lactis,* as a display control, and confirmed that this strain demonstrated no im-
217 provement in mucus binding (Figure 4d), again reiterating that the *L. reuteri* proteins enhance binding in a mucus-
218 specific manner.

219 The major mucus adhesin on EcN is considered to be the flagellum, formed with the structural subunit FliC
220 (Monteiro *et al.*, 2009). Additionally, EcN expresses a cellulose synthase (BscA) necessary for biofilm formation and
221 adhesion to epithelial cells (Friedlander, Vogel and Aizenberg, 2015). We sought to assess the role of FliC and
222 BcsA in EcN mucus binding. Somewhat unexpectedly, and counter to previous reports, deleting both genes
223 ($EcN^{\Delta fliC,\Delta bscA}$) increase the mucoadhesive ability of EcN (Figure 4g), shown by a curve shift up and to the left. This
224 relationship is reversed, however, when the adhesion of each strain was subsequently tested on polystyrene alone
225 (Figure S4a). Recently, the *E. coli* flagellum was shown to adhere more tightly to hydrophobic abiotic surfaces than
226 hydrophilic substrates and may in fact impede other surface adhesins as a tradeoff for mobility (Karlskås *et al.*,
227 2014). This behavior is consistent with our results in Figure 4g, suggesting the adhesion of EcN to the hydrophilic
228 mucus surface was improved by removing the flagellum, and it is possible that previous measurements of EcN
229 mucoadhesion were either confounded by the cells binding other available abiotic surfaces like plastic. These re-
230 sults emphasize the importance of covalently immobilizing mucus and measuring global binding parameters
231 across a wide range of cell concentrations. Beyond the initial observation that more $EcN^{\Delta fliC,\Delta bscA}$ cells remain
232 bound than EcN, the binding parameters show a stark difference in curve shape between the wild-type and
233 knockout strains, perhaps suggesting different mechanisms of adhesion (Table 2). This is further emphasized when
234 observing binding on polystyrene alone and with the observation that the removal of the flagellum improves
235 binding to PIM and BSA indiscriminately (Figure S4). Despite a 46% increase in adhesion at OD_{600} 0.5, $EcN^{\Delta fliC,\Delta bscA}$
236 retains a similar curve shape to EcN because nonspecific interactions dominate the adhesion of both cell types to
237 polystyrene (Figure S4a). Curve shapes are altered when protein-protein interactions (mucus-specific or otherwise)
238 at surfaces dominate (Figure 4h).

239 **CONCLUSIONS**

240 Our improved mucus adhesion assay isolates mucus-specific interactions by immobilizing a confluent layer of
241 mucus to a plate surface. This removes previously observed variability caused through non-specific adhesion
242 mechanisms to the polystyrene while retaining the benefits of a minimalistic adhesion assay. The assay is further
243 improved by implementing automated wash steps for consistency, and, measuring adhesion over a wide range of

244 cell concentrations facilitates the interpolation of a mucus-binding curve. Curve parameters offer a more global
245 metric for strain-specific mucoadhesion without the need to normalize to a reference strain. We observe clear
246 dose-dependent differences in the binding ability of a number of probiotic strains with the curve parameters ex-
247 tending these relationships beyond the traditional measurement of percent adhesion at one cell density. Im-
248 portantly, known and putative mucus-associated factors were expressed on the surface of a poor mucus binder, *L.*
249 *lactis* MG1363, and mucoadhesion was significantly altered, reinstating the mucus-specific interactions of these
250 cell-surface elements. Furthermore, a new understanding of EcN mucoadhesion was observed with the polar fla-
251 gellum, originally considered a major mucoadhesin, actually impeding mucus adhesion and more general hydro-
252 philic surface adhesion. This emphasizes the advantage of our updated assay over a traditional approach in which
253 nonspecific interactions with the abiotic plate surface likely confounded mucoadhesion measurements. These re-
254 sults offer promise in the delivery and control of drug-release in the emerging field of living microbial therapeu-
255 tics.

256 **SIGNIFICANCE**

257 This work presents an improved *in vitro* adhesion assay to determine mucus-specific adhesion mechanisms of
258 bacteria. The development of mucus-binding curves directly quantifies strain-specific dose-depending
259 mucoadhesion with curve parameters acting as a more universal metric for adhesion than the traditional percent
260 adhesion normalized to a reference strain. This work is a significant advancement for the delivery and control of
261 therapeutics through various probiotic chassis.

262 **ACKNOWLEDGEMENTS**

263 The authors would like to thank Dr. Huan-Hsuan Hsu and Prof. Xiaocheng Jiang for their advisement and re-
264 sources when developing the surface immobilization procedure. A special thanks to Josef R. Bober for his advise-
265 ment with surface-display in LAB. This work was financially supported by grant numbers R03HD090444 and
266 DP2HD091798 of the National Institutes of Health.

267

268 ## AUTHOR CONTRIBUTIONS

269 Z.J.S.M. performed all experiments. Z.J.S.M. and N.U.N. designed all experiments, analyzed the data, and wrote the
270 manuscript. T.C.C. performed gene deletions in EcN.

271 ## DECLARATION OF INTERESTS

272 The authors declare no competing interests

273

FIGURES & LEGENDS

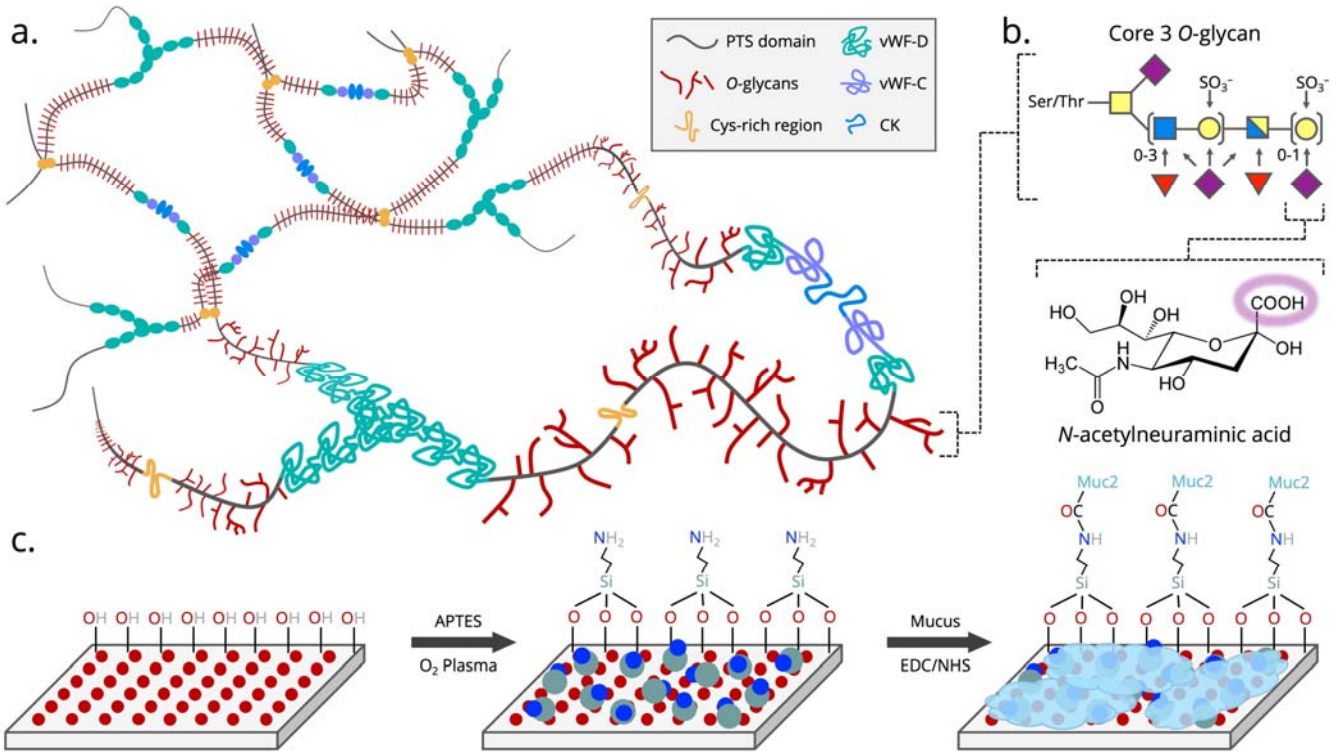

Figure 1. Schematic of mucus immobilization strategy

The structure of mucus presents an opportunity for covalent immobilization chemistry. Gel-forming mucins such as Muc2 form (a.) macromolecular sheets of trimers of dimers that crosslink or interact to form a mesh. Each mucin monomer has a highly glycosylated proline-threonine/serine (PTS) domain with the (b.) highly sialylated core 3 *O*-glycan dominating in the intestines. Sialic acid, or *N*-acetylneuraminic acid, provides a freely available carboxylic acid that can be (c.) coupled to a primary amine presented on a glass or plastic surface using EDC/NHS crosslinking chemistry.

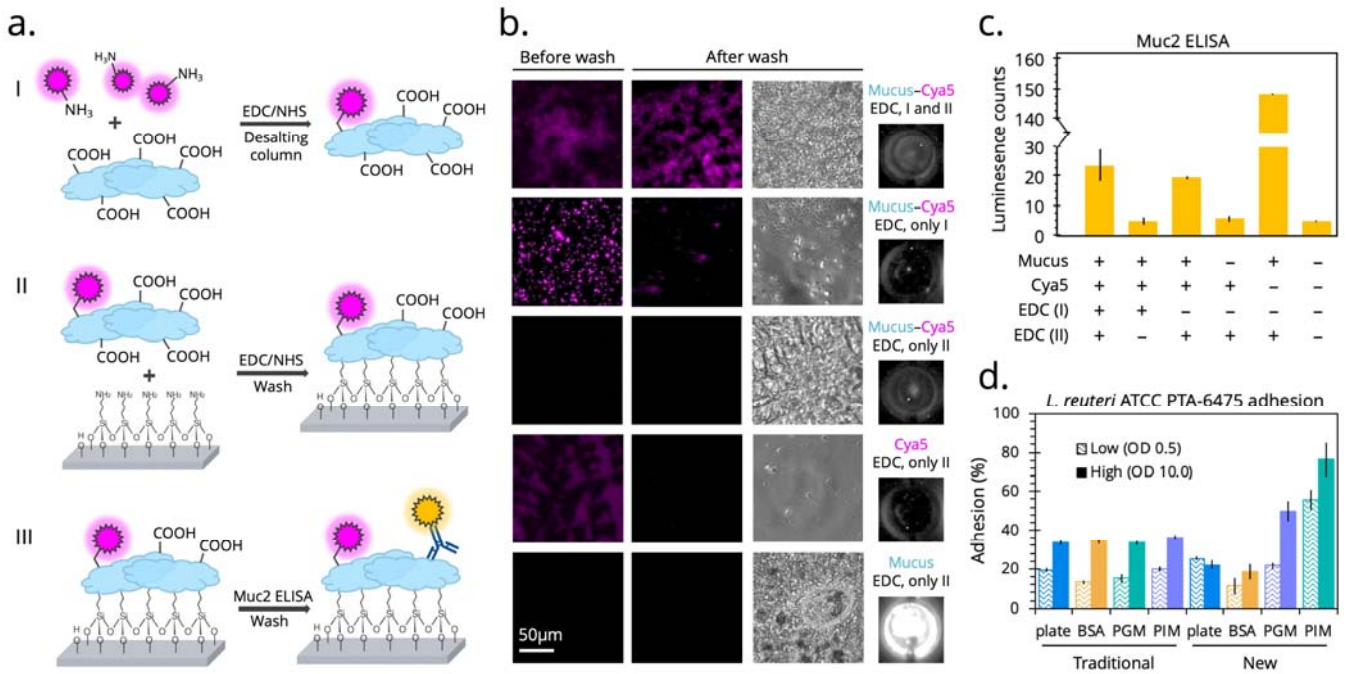

Figure 2. Validating the modified cell mucoadhesion assay and comparing to the traditional assay

(a.) Two EDC/NHS reactions were performed in tandem followed by a Muc2-specific ELISA to determine the success of the mucus immobilization. (b.) Fluorescence microscopy was then implemented to measure of the robustness and directionality of the coupling between mucus and sulfo-cyanine5 and between mucus and the plate surface. Each condition was imaged before and after vigorous washing and after the ELISA. (c.) Luminescence counts were quantified to determine mucus coverage, with the final optimized condition (1% PIM) measuring 10-fold higher than other conditions, as expected. (d.) With these final conditions, the traditional adhesion assay was compared to the newly optimized assay using the strong binder *L. reuteri* ATCC PTA-6475 as a metric for success on different protein surfaces.

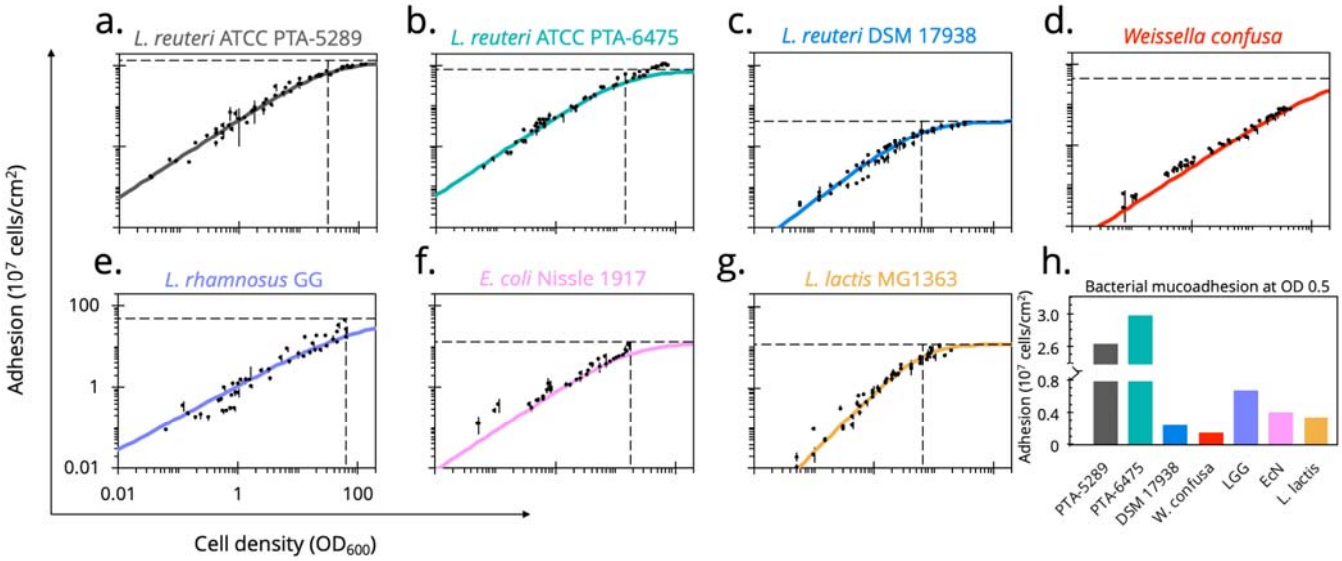

Figure 3. Dose-dependent mucus-binding curves for common probiotics

(a.-g.) Using our optimized plate assay, the number of cells adhered to immobilized mucus was measured over a large range of concentrations for common probiotics. Data points are reported as the mean values of quadruplicate wells across three independent experiments. Hill-type sigmoidal curves were fit, with curve parameters a metric for strain-specific mucoadhesive characteristics (Table 1). (h.) With the traditional assay typically performed at OD_{600} 0.5, comparative analysis across strains was visualized at this density.

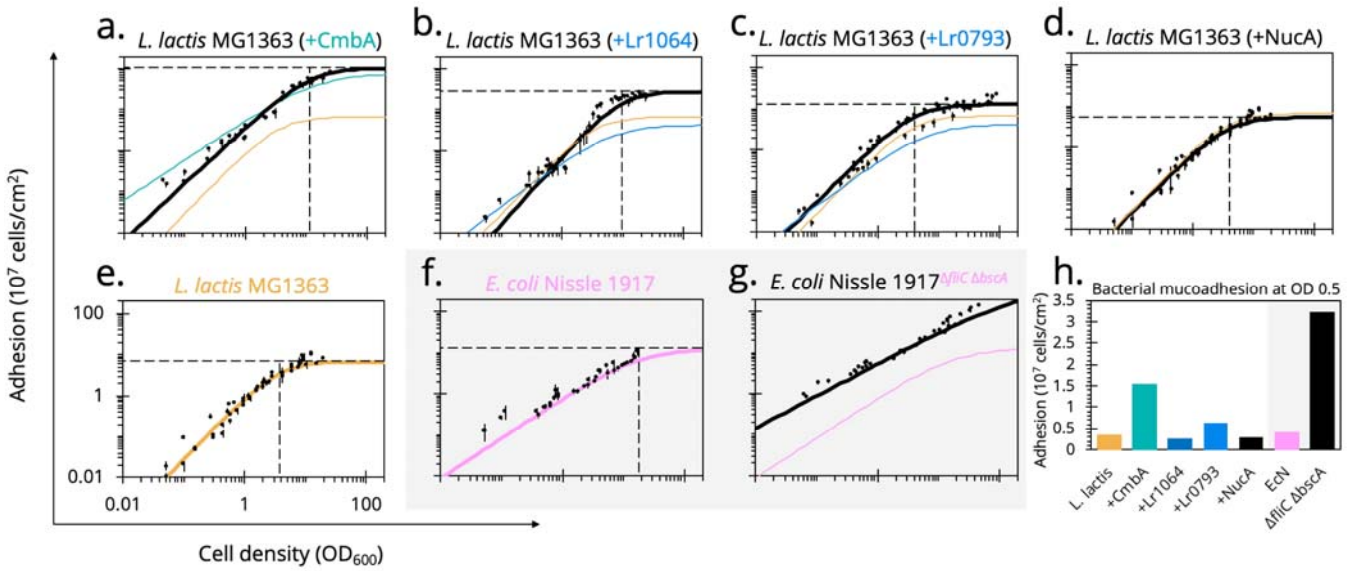

Figure 4. Altered dose-dependent mucoadhesion by heterologous protein expression

Known and putative mucus-associating surface proteins from *L. reuteri* were heterologously expressed in *L. lactis* MG1363. The (e.) wild-type *L. lactis* MG1363 binding curve (orange) was (a.-c.) compared to the engineered counterpart (black) as well as the *L. reuteri* strain from which the protein was sourced (green or blue). (d.) As a display control, an inactivated NucA^{E41Q} did not alter mucus binding compared to the wild-type strain. Alternatively, the flagellum of EcN, considered a known mucus-binding factor, and cellulose synthase, a contributor to biofilm formation, were (g.) knocked out but surprisingly improved mucoadhesion compared to the (f.) wild-type (pink). (h.) With the traditional assay typically performed at OD_{600} 0.5, comparative analysis across strains was visualized at this density.

313 **TABLES**

314 Table 1. Summary of mucus-binding curve parameters for common probiotics

Strain	[a]A_{max} ($\times 10^7$ cells/cm^2)	[b]OD_{A50}	n
L. reuteri ATCC PTA-6475	77.4 ± 3.1	14.3 ± 1.5	0.98 ± 0.05
L. reuteri ATCC PTA-5289	133.5 ± 7.5	30.0 ± 4.1	0.97 ± 0.05
L. reuteri DSM 17938	4.3 ± 0.3	6.2 ± 1.1	1.11 ± 0.11
Weissella confusa	44.7 ± 0.0	[a]203.7 ± 0.1	0.95 ± 0.001
L. rhamnosus GG	44.5 ± 0.3	[a]99.0 ± 0.8	0.80 ± 0.02
E. coli Nissle 1917	12.9 ± 0.2	17.7 ± 0.2	0.98 ± 0.04
L. lactis MG1363	6.8 ± 0.4	3.7 ± 0.4	1.52 ± 0.14

315

316 Parameters determined from sigmoidal curve fitting of experimental adhesion data, shown with 95% confidence
317 intervals

318 [a]Extrapolated value from curve fitting

319 [b]Standard curves to correlate OD_{600} to CFU/mL are reported for each strain in Table S1.

320

321

322 Table 2. Summary of mucus-binding curve parameters when altering mucoadhesive protein expression

Strain	[a]A_{max} ($\times 10^7$ cells/cm^2)	OD_{A50}	n
L. lactis MG1363	6.8 ± 0.4	3.7 ± 0.4	1.52 ± 0.14
+ $NucA^{E41Q}$	5.5 ± 0.4	4.0 ± 0.5	1.5 ± 0.13
+ CmbA	104.3 ± 4.6	11.5 ± 0.8	1.37 ± 0.12
+ Lr1064	27.8 ± 1.7	9.4 ± 0.9	1.64 ± 0.12
+ Lr0793	13.0 ± 0.5	4.1 ± 0.5	1.48 ± 0.22
E. coli Nissle 1917	12.9 ± 0.2	17.7 ± 0.2	0.98 ± 0.04
ΔfliC,ΔbscA	368.3 ± 5.5	[a]230.5 ± 3.6	0.78 ± 0.02

323

324 Parameters determined from sigmoidal curve fitting of experimental adhesion data, shown with 95% confidence
325 intervals

326 [a]Extrapolated value from curve fitting

327

328 **STAR ▯ METHODS**

329 **▯ EXPERIMENTAL MODEL AND SUBJECT DETAILS**

330 Microbial strains, plasmids, and growth conditions

331 All lactobacilli and *Weissella confusa* were cultured in de Man-Rogosa-Sharpe (MRS) medium (RPI Corp, Mt.
332 Prospect, IL) at 37 °C in static microaerobic conditions. *Lactococcus lactis* subsp. cremoris MG1363 was cultured in
333 GM17 medium (M17 broth (BD Difco, Franklin Lakes, NJ), 0.5 % (w/v) glucose) at 30 °C in static microaerobic con-
334 ditions. *E. coli* strains were cultured in lysogeny broth (LB) (VWR International, Randor, PA) at 37 °C with rotary
335 shaking at 250 rpm. All media was solidified using 1.5 % (w/v) agar (Teknova Inc, Hollister, CA). *E. coli* TG1*ΔendA*
336 was used as a host for the construction of the pSIP-based expression vectors listed in Table S2 and cultured as
337 above only supplemented with erythromycin (200 µg/mL) (RPI Corp). When *L. lactis* subsp. cremoris MG1363 was
338 used as hosts for these vectors, the strains were cultured as above only supplemented with erythromycin (5
339 µg/mL).

340 All cloning was performed in *E. coli* TG1$^{\Delta endA}$. Beginning with the plasmid pSIP411, the inducible promoter
341 PsppQ (Rud *et al.*, 2006) was replaced with the constitutive synthetic promoter P11 (Mathiesen *et al.*, 2009) using
342 the surrounding sites for restriction endonucleases BglII and NcoI. The genomic DNA of *L. reuteri* ATCC PTA-6475
343 and *L. reuteri* DSM 17938 were used as templates to amplify the known and putative mucus-associating factors in
344 this study using colony PCR. The pSIP411-P11 backbone, *lr1064*, and *lr0793* were digested with NcoI and XhoI
345 while *cmbA* was digested with PciI and XhoI. A site mutation was introduced into *nucA* using overlap PCR and the
346 inactive *nucA*^{E41Q} was inserted into a surface-display pSIP411-P11 variant (previously unpublished) by digestion
347 with NcoI and XmaI. This created a fusion construct of secretion signal peptide lp3050 (Fredriksen *et al.*, 2012), the
348 N-terminal LysM anchoring motif lp3014 (Fredriksen *et al.*, 2012), and *nucA*^{E41Q}. All cloning enzymes were pur-
349 chased from New England Biolabs (Ipswich, MA).

350

METHOD DETAILS

Transformation conditions

L. lactis MG1363 transformations require GSGM17 medium (GM17, 0.5 M sucrose, 2.5% (w/v) glycine). Electrocompetent cells were prepared by first growing in 5 mL GM17 overnight from a frozen stock optimized for GSGM17 growth. The resulting overnight was subcultured 1:9 in 10 mL GSGM17 and grown overnight. This final overnight culture was subcultured 1:7 in 40 mL GSGM17 and grown 6-7 h (OD_{600} 0.17). Cells were centrifuged at 3000 × g at 4 °C for 25 min and washed one in 40 mL ice-cold EP buffer (0.5 M sucrose, 10 % (w/v) glycerol). The cells were then suspended in 20 mL ice-cold EP buffer and incubated for 15 min on ice. Finally, cells were suspended in 400 µL ice-cold EP buffer and stored at −80 °C in 50 µL aliquots. To transform, 500 ng DNA, always diluted in dH2O to a final volume of 5 µL, was added to 50 µL electrocompetent cells and incubated on ice for 2 min. This mix was transferred to a pre-chilled 2 mm electroporation cuvette and electroporation was performed (2.0 kV, 25 µF, 200 Ω) using a Gene Pulser Xcell (Bio-Rad Laboratories, Hercules, CA) electroporation system. Cells were recovered by immediately adding 950 µL pre-warmed GM17 supplemented with recovery salts (20 mM $MgCl_2$, 2 mM $CaCl_2$) and incubating statically at 30 °C for 1.5 h. Cells were plated on selective GM17 with erythromycin (5 µg/mL) and grown for at least 24 h at 30 °C.

Isolation of primary porcine intestinal mucus

The intestines of 8-10-week-old pigs were obtained from a local supplier (Research 87 Inc, Boylston, MA). The small intestine was sectioned into 60 cm segments, squeezed of chyme, and placed in ice-cold phosphate buffered saline (PBS) (137 mM NaCl, 2.7 mM KCl, 10 mM Na_2HPO_4, 2 mM KH_2PO_4, pH 7.4). Each section was then splayed longitudinally, washed by dipping into a tray of ice-cold PBS, and moved to a second tray of ice-cold PBS. Pinning one end of an intestinal segment, a silicone spatula was used to scrape the mucus layer, placing the mucus in a beaker of ice-cold PBS. The crude PIM was centrifuged at 11000 × g at 4 °C for 10 min, and the supernatant was centrifuged again at 26000 × g at 4 °C for 15 min using an Optima L-90K (Beckman Coulter, Brea, CA)

374 ultracentrifuge with a 70-Ti fixed angle rotor (Beckman Coulter). This clarified PIM supernatant was then lyophi-
375 lized and stored at 4 °C.

376 Plate surface functionalization

377 The wells of 96-well clear polystyrene U-bottom (Greiner Bio-One, Kremsmünster, Austria) microtiter plates
378 were activated by oxygen plasma etching using a PE-200 (Plasma Etch, Inc. Carson City, NV) industrial benchtop
379 plasma processing system with a R301 RF Generator (Seren IPS, Inc., Vineland, NJ) power supply (105 W, 1 min
380 plasma time, 50 psi vacuum pressure, 20 cc/min O_2 flow). Immediately, 200 µL of APTES (5% v/v in ethanol) was
381 added to each well, and the plate was sealed with parafilm and incubated at room temperature for 15 min. The
382 plate was then washed twice with ethanol and dried with an air stream, always minimizing exposure to humidity or
383 water. A 1% PIM solution was prepared in PBS. Separately, a 10x solution of EDC (Thermo Fisher Scientific, Wal-
384 tham, MA) was made in PBS. The EDC was added to the 1% PIM to a final concentration of 5 mM and placed on a
385 rocker for 5 min. During this time, NHS (TCI Chemicals, Portland, OR) was weighed out and added to the 1% PIM
386 to a final concentration of 10 mM, again using a rocker to mix for 5 min. Finally, 200 µL of the PIM/EDC/NHS was
387 added to each well of the APTES functionalized plate. The plate was then sealed with parafilm and incubated at
388 room temperature for 2 h before being left at 4 °C overnight.

389 Fluorescence microscopy, ELISA, and Western blot analysis

390 A coupling reaction was prepared as described in the "Plate surface functionalization" section above with a 1%
391 PIM solution combined with EDC/NHS and mixed for 5 min. Sulfo-cyanine5 amine (cya5) (Lumiprobe, Hunt Valley,
392 MA) was added to a final concentration of 1 mg/mL, and the reaction was incubated for 2 h at room temperature,
393 wrapped in foil to prevent light exposure. A Zeba spin desalting column (Thermo Fisher Scientific) was then used
394 to remove excess fluorophore. The mucus-cya5 conjugate was then used in a second coupling reaction, conjugat-
395 ing the mucus to a 96-well clear polystyrene U-bottom (Greiner Bio-One) microtiter plate. After a 2 h incubation,
396 excess volume was aspirated from each well condition. Microscope images were captured using a DMi8 (Leica Mi-
397 crosystems, Inc., Buffalo Grove, IL) microscope with 100x objective. Phase contrast images were taken with 1 ms

398 exposure. Fluorescent images were taken by exciting with a Y5 filter cube with 400 ms exposure and gain set to 4
399 on LAS X (Leica Microsystems, Inc.) software. Wells were then washed three times with a plate washer as described
400 in the "Mucus adhesion assay" section below.

401 Microscope images were again taken before an ELISA assay was performed. Each well was blocked for 1 h with
402 cold blocking buffer (5% (w/v) skim milk powder in TBST (20 mM Tris, 150 mM NaCl, 0.1% (v/v) Tween, pH 7.6)).
403 Wells were then washed three times with ice cold TBST, shaking at 150 rpm for 5 min each time. Wells were resus-
404 pended in 200 µL blocking buffer containing 0.1 µg rabbit anti-Muc2 (MyBioSource, Inc., San Diego, CA) primary
405 antibody and incubated on ice with shaking at 150 rpm for 1 h. After another three washes, the wells were resus-
406 pended in 200 µL blocking buffer containing 0.04 µg goat anti-rabbit IgG-HRP (Abcam, Cambridge, MA) second-
407 ary antibody and incubated on ice with shaking at 150 rpm for 30 min. Using a SuperSignal West Femto (Thermo
408 Fischer Scientific) chemiluminescence detection kit, images and luminescence values were recorded after 30 s ex-
409 posure on a UVP ChemiDoc-It2 810 (Analytik Jena US, LLC., Upland, CA) imager on VisionWorks LS (Analytik Jena
410 US, LLC) analysis software.

411 Flow cytometry

412 Five milliliter cultures of *L. lactis* MG1363 wild-type or carrying expression vectors were grown overnight as
413 described in the "Microbial strains, plasmids, and growth conditions" section above. Cells were centrifuged at 3000
414 × g for 5 min and washed twice with PBS before being suspended at OD_{600} 1.0. A 200 µL aliquot was resuspended
415 in 200 µL PBSA (2% (w/v) BSA in PBS) and incubated on ice for 30 min. The cells were then resuspended in 50 µL
416 PBSA containing 1 µg mouse anti-6xHis (Thermo Fisher Scientific) primary antibody and incubated for 1 h at room
417 temperature. The cells were washed three times with PBSA before being suspended in 50 µL PBSA containing 0.4
418 µg goat anti-mouse IgG-AlexaFluor488 (Thermo Fisher Scientific) secondary antibody and incubated for 15 min on
419 ice, wrapped in foil to prevent light exposure. Finally, the cells were washed three times with PBSA and suspended
420 in 500 µL PBSA. Samples were run on an Attune NxT (Thermo Fisher Scientific) flow cytometer, using a 50 mW
421 blue laser to collect at least 10,000 events. Histograms were analyzed on FCS Express 6 (De Novo Software, Glen-
422 dale, CA) software.

423 ## Gene knockouts in *E. coli* Nissle 1917

424 Antibiotic cassette insertion and gene knockout (KO) were performed using lambda red recombineering
425 (Datsenko and Wanner, 2000). Kanamycin (kan), chloramphenicol (cat), and ampicillin (amp) were used at 50, 25,
426 and 100 µg/mL, respectively, to maintain plasmids or select for integration of resistance cassettes. Amplification of
427 the cat cassette from pKD3 was used for *bcsA* KO, while amplification of the kan cassette from pKD4 was used for
428 *fliC* KO. Verification of antibiotic resistance cassette integration and removal was verified by Taq colony PCR.
429 Plasmid curing and cassette removal was verified by absence of growth on LB agar plates. All primers for cassette
430 amplification and removal verification are listed in the ★ Key Resources Table.

431 ## Fluorescent labelling of bacteria

432 All strains were grown to early stationary phase in 200 mL of their respective growth media (approximately 10
433 h for LAB strains). To promote flagellum expression *E. coli* was grown for 24 h at 30 °C at 85 rpm. Cells were then
434 centrifuged at 3000 × g at 4 °C for 10 min and washed three times with 50 mL PBS. Cells were then diluted in PBS
435 to OD_{600} 1.0 and labelled by the addition of carboxyfluorescein diacetate (cFDA) (Thermo Fisher Scientific) to a
436 final concentration of 10 µM by incubating at 37 °C for 40 min with rotary shaking at 85 rpm. Again,
437 carboxyfluorescein (cF)-labelled cells were washed three times as above and suspended in 10 mL PBS.

438 ## Mucus adhesion assay

439 Cells were diluted using PBS from the 10 mL stock to OD_{600} values approximately evenly-spaced across three
440 orders of magnitude. The mucus solution left after plate functionalization was removed from the microtiter plate
441 by aspiration. Two hundred microliters of each dilution were plated in four technical replicates. A separate 225 µL
442 of each OD_{600} dilution was placed in microfuge tubes, and both the plate and tubes were then incubated at 37 °C
443 for 4 h with rotary shaking at 500 rpm. Using an AquaMax4000 (Molecular Devices, San Jose, CA) plate washer
444 with a cell wash head, the plate was washed three times with PBS (center aspiration 50 µL/well/s; wall dispense 7.2
445 mL/plate/s; probe height 3 mm) ending with a final aspiration step. The adhered cells were lysed by adding 200 µL
446 lysis buffer (1% (w/v) SDS, 0.1 M NaOH) and incubating at 37 °C for 1 h with rotary shaking at 750 rpm. Addition-

447 ally, the 225 µL cell dilutions were centrifuged at 5000 × g for 5 min and suspended in lysis buffer as fluorescence
448 controls. All lysates were transferred to a 96-well F-bottom black FluoTrac (Greiner Bio-One) microtiter plate. The
449 plate was passed over with a flame to remove bubbles and fluorescence was measured (Em/485 nm, Ex/520 nm)
450 using a SpectraMax M3 (Molecular Devices) plate reader. Blank wells containing only lysis buffer were used for
451 background subtraction.

452 ## QUANTIFICATION AND STATISTICAL ANALYSIS

453 ### Adhesion curve fitting and statistical analysis

454 Plate data was background corrected by subtracting the relative fluorescence units (RFU) of blank wells con-
455 taining only lysis buffer. The means of experimental replicates were used for further data analysis. By plotting the
456 standards as RFU vs OD_{600}, the slope of a linear trend (C_1) was used to associate RFU per unit OD_{600}. This relation-
457 ship, along with the volume-to-surface-area relationship (V/A) derived from a microtiter plate schematic (Figure
458 S5) and the CFU/mL per OD_{600} (C_2), can be used to convert values to adhered cells per unit area (A_y):

$$A_y = (RFU_y)(C_1{}^{-1})(C_2)(\frac{V}{A})$$

459 Values for C1 and C2 are summarized in Table S1. A typical sigmoidal (Hill-type) curve was adapted to model fit
460 cell adhesion:

$$A_y = \frac{A_{max} OD_y^n}{OD_{A50}^n + OD_y^n}$$

461 Here, A_y is the adhered cells per unit area at cell concentration y, A_{max} is the maximum possible adhered cells per
462 unit area, OD is the OD_{600} for cell concentration y, OD_{A50} is the OD_{600} required for half the maximum number of
463 cells to adhere to the well, and n is the sigmoid factor. The curve parameters were obtained by using the nonlinear
464 curve fitting function in MATLAB (fitnlm) with robust bi-square least squares regression analysis, which applies a
465 weighting factor to discount outliers. Plots of cells per unit area versus OD_{600} were created to visualize the adhe-
466 sion differences between strains.

467 ## KEY RESOURCES TABLE

468 ## SUPPLEMENTAL INFORMATION

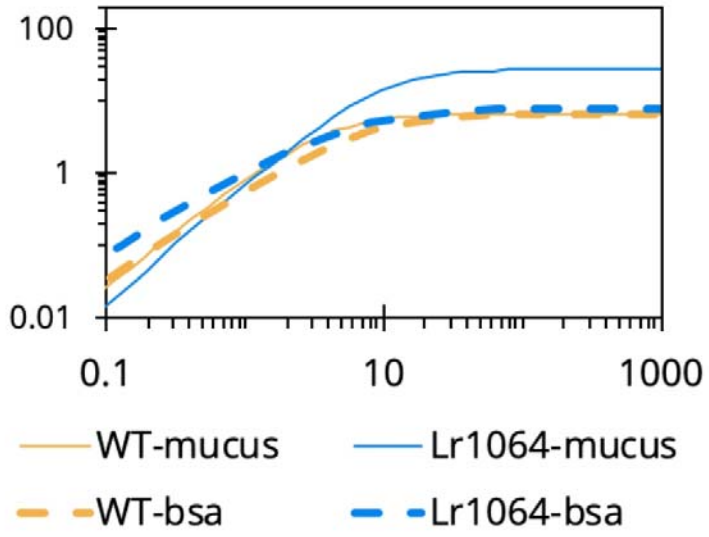

469

470 Figure S1. Adhesion of *L. lactis* MG1363 to different substrates

471 The observed increase in adhesion of *L. lactis* MG1363 when expressing Lr1064 is shown to be specific to mucus;
472 adhesion does not improve over wild-type *L. lactis* MG1363 when both are adhered to BSA. Only the curve fit is
473 shown for clarity.

474

475

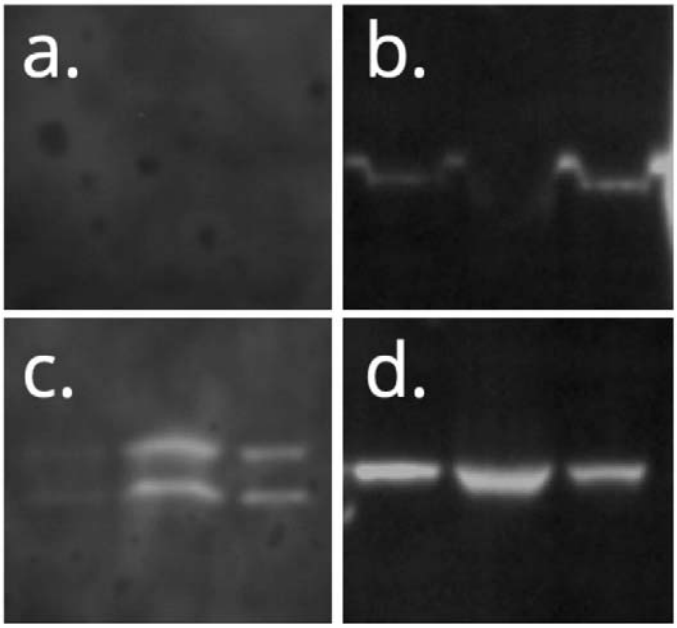

476 Figure S2. Western blots to confirm recombinant expression of mucus-associated factors

477 His-tag fused (a.) empty vector, (b.) CmbA, (c.) Lr0793, and (d.) Lr1064 were expressed in *L. lactis* MG1363. Bands
478 show the surface-stripped, soluble, and insoluble fractions. Proteins expressed at the correct size (ladder not
479 shown).

480

481

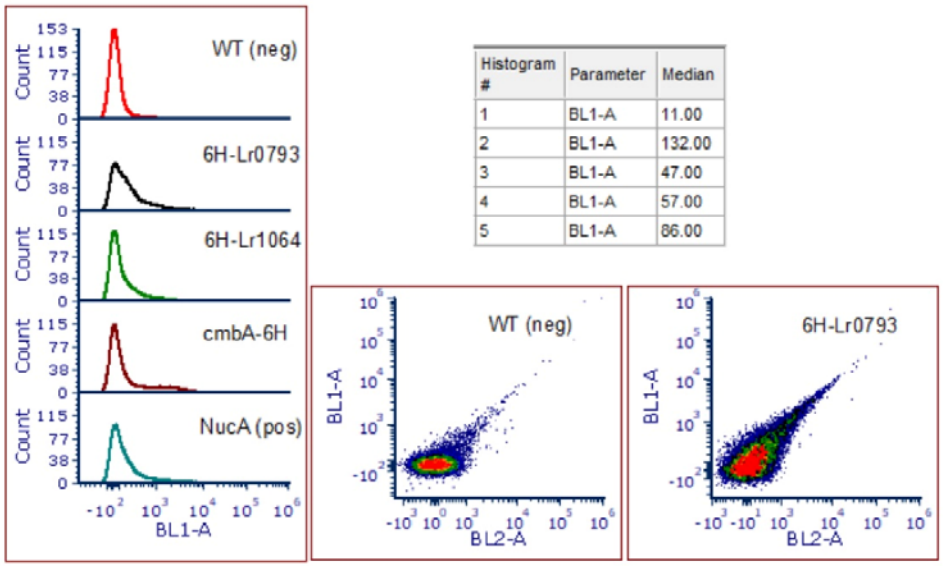

Histogram #	Parameter	Median
1	BL1-A	11.00
2	BL1-A	132.00
3	BL1-A	47.00
4	BL1-A	57.00
5	BL1-A	86.00

482

483 Figure S3. Flow-cytometry confirms surface display of recombinant mucus-associated factors

484 His-tag fused mucus-associated factors were labelled with AlexaFluor488 conjugated anti-His-tag antibody. Wild-
485 type *L. lactis* MG1363 was used as a negative control and inactivated NucA^{E41Q} was used as a positive control for
486 surface display. A shift to the right on each histogram is an increase in fluorescence, correlated to protein display.
487 Median fluorescence units are shown in the table for each corresponding histogram.

488

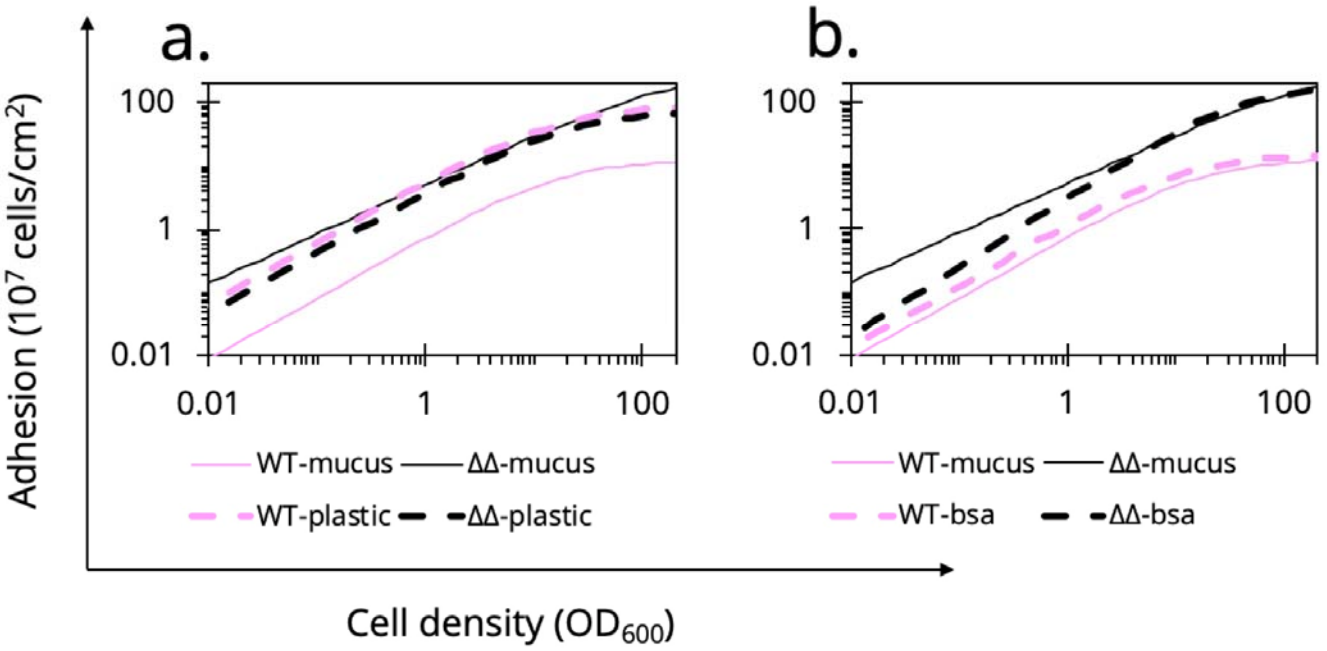

Figure S4. Adhesion of *E. coli* Nissle 1917 to different substrates

While the deletion of FliC and BscA increased the ability of EcN to bind to mucus, (a.) the relationship was the reverse when adherence of wild-type EcN and EcN$^{\Delta fliC,\Delta bscA}$ was quantified on uncoated polystyrene. (b.) Further investigation shows that EcN$^{\Delta fliC,\Delta bscA}$ seems to indiscriminately bind hydrophilic surfaces as adhesion was increased on mucus and BSA.

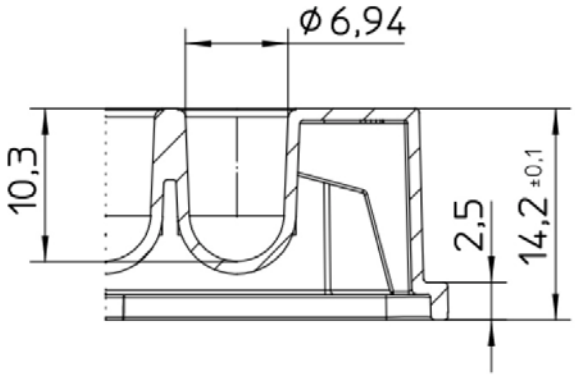

Figure S5. Schematic of Greiner U-bottom plate geometry

Sourced from Greiner 96-Well U-bottom product document and used to calculate well surface area

502 Table S1. Linear relationships between RFU and OD_{600} and OD_{600} and CFU/mL for each strain

	RFU/OD_{600}	CFU/mL ($\times 10^8$) per OD_{600}
L. reuteri ATCC PTA-5289	3109	3.7
L. reuteri ATCC PTA-6475	2794	3.3
L. reuteri DSM 17938	2334	6.7
W. confusa	397	3.8
L. rhamnosus GG	1002	1.4
E. coli Nissle 1917	51	8.0
L. lactis MG1363	7005	6.8

503

504 Values for CFU/mL acquired by growing cells overnight, checking the OD_{600} of three dilutions, and plating a
505 10,000x dilution of those concentrations to count CFUs.

506

507 **ABBREVIATIONS**

508 ABC, ATP-binding cassette

509 APTES, (3-aminopropyl)triethoxysilane

510 BSA, bovine serum albumin

511 BscA, cellulose synthase catalytic subunit A

512 cFDA, carboxyfluorescein diacetate

513 CmbA, cell and mucus binding protein A

514 CnBP, collagen binding protein

515 EcN, *E. coli* Nissle 1917

516 EDC, *N*-ethyl-*N'*-(3-dimethyl-aminopropyl) carbodiimide

517 ELISA, enzyme-linked immunosorbent assay

518 EPS, extracellular polysaccharide

519 FU. 5-fluorouracil

520 GI, gastrointestinal

521 IEC, intestinal epithelial cell

522 LAB, lactic acid bacteria

523 MapA, mucus adhesion promoting protein A

524 MTX, methotrexate

525 NHS, *N*-hydroxysuccinimide

526 NucA, nuclease A

527 PGM, porcine gastric mucus

528 PIM, porcine intestinal mucus

529 PTS, proline-threonine/serine

530 RFU, relative fluorescence unit

531

532 **REFERENCES**

533 Aleljung, P. *et al.* (1994) "Purification of collagen-binding proteins of Lactobacillus reuteri NCIB 11951," *Current*
534 *Microbiology*, 28(4). doi: 10.1007/BF01575966.

535 Anderson, G. G. *et al.* (2003) "Intracellular bacterial biofilm-like pods in urinary tract infections," *Science*, 301(5629).
536 doi: 10.1126/science.1084550.

537 Ayeni, F. A. *et al.* (2011) "Evaluation of the functional potential of Weissella and Lactobacillus isolates obtained
538 from Nigerian traditional fermented foods and cow's intestine," *International Journal of Food Microbiology*. Elsevier
539 B.V., 147(2), pp. 97–104. doi: 10.1016/j.ijfoodmicro.2011.03.014.

540 Båth, K. *et al.* (2005) "The cell surface of Lactobacillus reuteri ATCC 55730 highlighted by identification of 126 ex-
541 tracellular proteins from the genome sequence," *FEMS Microbiology Letters*. Oxford, UK: Elsevier B.V, 253(1). doi:
542 10.1016/j.femsle.2005.09.042.

543 Bober, J. R., Beisel, C. L. and Nair, N. U. (2018) "Synthetic Biology Approaches to Engineer Probiotics and Members
544 of the Human Microbiota for Biomedical Applications," (March), pp. 277–300.

545 Boekhorst, J. *et al.* (2006) "Comparative analysis of proteins with a mucus-binding domain found exclusively in lac-
546 tic acid bacteria," *Microbiology*. England: Soc General Microbiol, 152(1). doi: 10.1099/mic.0.28415-0.

547 Caldara, M. *et al.* (2012) "Mucin biopolymers prevent bacterial aggregation by retaining cells in the free-swimming
548 state," *Current Biology*. Elsevier Ltd, 22(24). doi: 10.1016/j.cub.2012.10.028.

549 Celli, J. P. *et al.* (2007) "Rheology of gastric mucin exhibits a pH-dependent sol-gel transition," *Biomacromolecules*,
550 8(5). doi: 10.1021/bm0609691.

551 Cho, I. and Blaser, M. J. (2012) "The human microbiome: at the interface of health and disease.," *Nature Reviews*
552 *Genetics*, 13(4). doi: 10.1038/nrg3182.

553 Chowdhury, S. *et al.* (2019) "Programmable bacteria induce durable tumor regression and systemic antitumor im-
554 munity," *Nature Medicine*. Springer US, 25(July). doi: 10.1038/s41591-019-0498-z.

555 Coyte, K. Z., Schluter, J. and Foster, K. R. (2015) "The ecology of the microbiome: Networks, competition, and sta-
556 bility.," *Science*, 350(6261). doi: 10.1126/science.aad2602.

557 Danino, T. *et al.* (2015) "Programmable probiotics for detection of cancer in urine," *Science Translational Medicine*,
558 7(289), p. 289ra84. doi: 10.1126/scitranslmed.aaa3519.

559 Datsenko, K. A. and Wanner, B. L. (2000) "One-step inactivation of chromosomal genes in Escherichia coli K-12
560 using PCR products," *Proceedings of the National Academy of Sciences*, 97(12), pp. 6640–6645. doi:
561 10.1073/pnas.120163297.

562 Derrien, M. and van Hylckama Vlieg, J. E. T. (2015) "Fate, activity, and impact of ingested bacteria within the human
563 gut microbiota," *Trends in Microbiology*. Elsevier Ltd, 23(6). doi: 10.1016/j.tim.2015.03.002.

564 Douillard, F. P. and de Vos, W. M. (2014) "Functional genomics of lactic acid bacteria: From food to health," *Micro-*
565 *bial Cell Factories*. BioMed Central Ltd, 13(Suppl 1). doi: 10.1186/1475-2859-13-S1-S8.

566 Etzold, S. *et al.* (2014) "Structural and molecular insights into novel surface exposed mucus adhesins from Lacto-
567 bacillus reuteri human strains," *Molecular Microbiology*. HOBOKEN: WILEY-BLACKWELL, 92(3). doi:
568 10.1111/mmi.12574.

569 Fabich, A. J. *et al.* (2008) "Comparison of carbon nutrition for pathogenic and commensal Escherichia coli strains in
570 the mouse intestine," *Infection and Immunity*, 76(3), pp. 1143–1152. doi: 10.1128/IAI.01386-07.

571 Fairfax, M. R., Lephart, P. R. and Salimnia, H. (2014) "Weissella confusa: Problems with identification of an oppor-
572 tunistic pathogen that has been found in fermented foods and proposed as a probiotic," *Frontiers in Microbiology*,
573 5(JUN), pp. 1–5. doi: 10.3389/fmicb.2014.00254.

574 Fredriksen, L. *et al.* (2012) "Surface display of N-terminally anchored invasin by Lactobacillus plantarum activates
575 NF-κB in monocytes," *Applied and Environmental Microbiology*, 78(16). doi: 10.1128/aem.01227-12.

576 Friedlander, R. S., Vogel, N. and Aizenberg, J. (2015) "Role of flagella in adhesion of Escherichia coli to abiotic sur-
577 faces," *Langmuir*, 31(22). doi: 10.1021/acs.langmuir.5b00815.

578 Gionchetti, P. *et al.* (2003) "Prophylaxis of pouchitis onset with probiotic therapy: A double-blind, placebo-
579 controlled trial," *European Journal of Gastroenterology and Hepatology*, 15(7). doi: 10.1097/00042737-200307000-
580 00020.

581 Hancock, V., Dahl, M. and Klemm, P. (2010) "Probiotic Escherichia coli strain Nissle 1917 outcompetes intestinal
582 pathogens during biofilm formation," *Journal of Medical Microbiology*, 59(4). doi: 10.1099/jmm.0.008672-0.

583 Hill, A. v (1910) "The possible effects of aggregation of haemoglobin on its dissociation curves," *J. Physiol. London*,
584 40.

585 Hwang, I. Y. *et al.* (2017) "Engineered probiotic Escherichia coli can eliminate and prevent Pseudomonas
586 aeruginosa gut infection in animal models," *Nature Communications*. Nature Publishing Group, 8. doi:
587 10.1038/ncomms15028.

588 Hyland, N. and Stanton, C. (2016) *The gut-brain axis: Dietary, probiotic, and prebiotic interventions on the*
589 *microbiota*. London, UK□: Academic Press is an imprint of Elsevier.

590 Isabella, V. M. *et al.* (2018) "Development of a synthetic live bacterial therapeutic for the human metabolic disease
591 phenylketonuria," *Nature Biotechnology*. Nature Publishing Group, 36(August), pp. 857–867. doi: 10.1038/nbt.4222.

592 Jenkinson, H. F. (1994) "Cell surface protein receptors in oral streptococci," *FEMS Microbiology Letters*, 121(2). doi:
593 10.1111/j.1574-6968.1994.tb07089.x.

594 Jensen, H. *et al.* (2012) "In vitro testing of commercial and potential probiotic lactic acid bacteria," *International*
595 *Journal of Food Microbiology*, 153(1–2). doi: 10.1016/j.ijfoodmicro.2011.11.020.

596 Jensen, H. *et al.* (2014) "Role of Lactobacillus reuteri cell and mucus binding protein A (CmbA) in adhesion to in-
597 testinal epithelial cells and mucus in vitro," *Microbiology (United Kingdom)*, 160(PART 4). doi:
598 10.1099/mic.0.073551-0.

599 Joeres-Nguyen-Xuan, T. H. *et al.* (2010) "Survival of the probiotic Escherichia coli Nissle 1917 (EcN) in the gastroin-
600 testinal tract given in combination with oral mesalamine to healthy volunteers," *Inflammatory Bowel Diseases*,
601 16(2). doi: 10.1002/ibd.21042.

602 Jonsson, H., Ström, E. and Roos, S. (2001) "Addition of mucin to the growth medium triggers mucus-binding activi-
603 ty in different strains of Lactobacillus reuteri in vitro," *FEMS Microbiology Letters*, 204(1). doi: 10.1016/S0378-
604 1097(01)00369-X.

605 Kankainen, M. *et al.* (2009) "Comparative genomic analysis of Lactobacillus rhamnosus GG reveals pili containing a
606 human-mucus binding protein," *Proc Natl Acad Sci U S A*, 106(40). doi: 10.1073/pnas.0908876106.

607 Karlskås, I. L. *et al.* (2014) "Heterologous protein secretion in lactobacilli with modified pSIP vectors," *PLoS One*.
608 San Francisco: Public Library of Science, 9(3). doi: 10.1371/journal.pone.0091125.

609 Khalili, A. A. and Ahmad, M. R. (2015) "A review of cell adhesion studies for biomedical and biological applica-
610 tions," *International Journal of Molecular Sciences*, 16(8). doi: 10.3390/ijms160818149.

611 Koropatkin, N. M., Cameron, E. A. and Martens, E. C. (2012) "How glycan metabolism shapes the human gut
612 microbiota," *Nature Reviews Microbiology*, 10(5). doi: 10.1038/nrmicro2746.

613 Krishnan, S. *et al.* (2018) "Gut Microbiota-Derived Tryptophan Metabolites Modulate Inflammatory Response in
614 Hepatocytes and Macrophages," *Cell Reports*. ElsevierCompany., 23(4). doi: 10.1016/j.celrep.2018.03.109.

615 Laparra, J. M. and Sanz, Y. (2009) "Comparison of in vitro models to study bacterial adhesion to the intestinal epi-
616 thelium," *Letters in Applied Microbiology*, 49(6). doi: 10.1111/j.1472-765X.2009.02729.x.

617 Larsson, J. M. H. *et al.* (2009) "A complex, but uniform O-glycosylation of the human MUC2 mucin from colonic
618 biopsies analyzed by nanoLC/MSn," *Glycobiology*, 19(7). doi: 10.1093/glycob/cwp048.

619 Lasaro, M. A. *et al.* (2009) "F1C fimbriae play an important role in biofilm formation and intestinal colonization by
620 the escherichia coli commensal strain nissle 1917," *Applied and Environmental Microbiology*, 75(1). doi:
621 10.1128/AEM.01144-08.

622 Latousakis, D. *et al.* (2019) "Serine-rich repeat protein adhesins from Lactobacillus reuteri display strain specific
623 glycosylation profiles," *Glycobiology*, 29(1). doi: 10.1093/glycob/cwy100.

624 Le, D. T. L. *et al.* (2013) "Unraveling the role of surface mucus-binding protein and pili in muco-adhesion of
625 Lactococcus lactis," *PLoS ONE*, 8(11). doi: 10.1371/journal.pone.0079850.

626 Lebeer, S. *et al.* (2009) "Identification of a gene cluster for the biosynthesis of a long, galactose-rich
627 exopolysaccharide in Lactobacillus rhamnosus GG and functional analysis of the priming glycosyltransferase," *Ap-*
628 *plied and Environmental Microbiology*, 75(11). doi: 10.1128/AEM.02919-08.

629 Lee, Y. K. *et al.* (2000) "Quantitative approach in the study of adhesion of lactic acid bacteria to intestinal cells and
630 their competition with enterobacteria," *Applied and Environmental Microbiology*, 66(9). doi:
631 10.1128/AEM.66.9.3692-3697.2000.

632 Leteurtre, E. *et al.* (2004) "Differential mucin expression in colon carcinoma HT-29 clones with variable resistance
633 to 5-fluorouracil and methotrexate," *Biology of the Cell*, 96(2). doi: 10.1016/j.biolcel.2003.12.005.

634 Li, X. J. *et al.* (2008) "The adhesion of putative probiotic lactobacilli to cultured epithelial cells and porcine intesti-
635 nal mucus," *Journal of Applied Microbiology*. Blackwell Publishing Ltd, 104(4). doi: 10.1111/j.1365-
636 2672.2007.03636.x.

637 MacKenzie, D. A. *et al.* (2010) "Strain-specific diversity of mucus-binding proteins in the adhesion and aggregation
638 properties of Lactobacillus reuteri," *Microbiology*. England: Society for General Microbiology, 156(11). doi:
639 10.1099/mic.0.043265-0.

640 Mackie, A. R. *et al.* (2017) "Innovative Methods and Applications in Mucoadhesion Research," *Macromolecular Bio-*
641 *science*, 17(8). doi: 10.1002/mabi.201600534.

642 Maltby, R. *et al.* (2013) "Nutritional Basis for Colonization Resistance by Human Commensal Escherichia coli Strains
643 HS and Nissle 1917 against E. coli O157:H7 in the Mouse Intestine," *PLoS ONE*, 8(1). doi:
644 10.1371/journal.pone.0053957.

645 Mathiesen, G. *et al.* (2009) "Genome-wide analysis of signal peptide functionality in Lactobacillus plantarum
646 WCFS1," *BMC Genomics*, 10. doi: 10.1186/1471-2164-10-425.

647 Mays, Z. J. and Nair, N. U. (2018) "Synthetic biology in probiotic lactic acid bacteria: At the frontier of living thera-
648 peutics," *Current Opinion in Biotechnology*. Elsevier Ltd, 53, pp. 224–231. doi: 10.1016/j.copbio.2018.01.028.

649 Mennigen, R. *et al.* (2009) "Probiotic mixture VSL#3 protects the epithelial barrier by maintaining tight junction
650 protein expression and preventing apoptosis in a murine model of colitis," *American Journal of Physiology-*
651 *Gastrointestinal and Liver Physiology*, 296(5). doi: 10.1152/ajpgi.90534.2008.

652 Monteiro, C. *et al.* (2009) "Characterization of cellulose production in Escherichia coli Nissle 1917 and its biological
653 consequences," *Environmental Microbiology*, 11(5). doi: 10.1111/j.1462-2920.2008.01840.x.

654 Mukherjee, S. and Ramesh, A. (2015) "Bacteriocin-producing strains of Lactobacillus plantarum inhibit adhesion of
655 Staphylococcus aureus to extracellular matrix: Quantitative insight and implications in antibacterial therapy," *Jour-*
656 *nal of Medical Microbiology*, 64(12). doi: 10.1099/jmm.0.000181.

657 Nishiyama, K., Sugiyama, M. and Mukai, T. (2016) "Adhesion Properties of Lactic Acid Bacteria on Intestinal Mucin,"
658 *Microorganisms*, 4(4). doi: 10.3390/microorganisms4030034.

659 Oh, P. L. *et al.* (2010) "Diversification of the gut symbiont lactobacillus reuteri as a result of host-driven evolution,"
660 *ISME Journal*. England: Nature Publishing Group, 4(3). doi: 10.1038/ismej.2009.123.

661 Ollech, J. E. *et al.* (2016) "Use of probiotics in prevention and treatment of patients with Clostridium difficile infec-
662 tion," *Best Practice and Research: Clinical Gastroenterology*. Baillière Tindall, 30(1). doi: 10.1016/j.bpg.2016.01.002.

663 Ou, B. *et al.* (2016) "Genetic engineering of probiotic Escherichia coli Nissle 1917 for clinical application," *Applied*
664 *Microbiology and Biotechnology*. Applied Microbiology and Biotechnology, 100(20). doi: 10.1007/s00253-016-
665 7829-5.

666 Ouwehand, A. C. (2017) "A review of dose-responses of probiotics in human studies," *Beneficial Microbes*, 8(2). doi:
667 10.3920/BM2016.0140.

668 Petrova, M. I. *et al.* (2016) "The lectin-like protein 1 in Lactobacillus rhamnosus GR-1 mediates tissue-specific ad-
669 herence to vaginal epithelium and inhibits urogenital pathogens," *Scientific Reports*. Nature Publishing Group,
670 6(October). doi: 10.1038/srep37437.

671 Riglar, D. T. *et al.* (2017) "Engineered bacteria can function in the mammalian gut long-term as live diagnostics of
672 inflammation," *Nature Biotechnology*, 35(7), pp. 653–658. doi: 10.1038/nbt.3879.

673 Rojas, M., Ascencio, F. and Conway, P. L. (2002) "Purification and Characterization of a Surface Protein from Lacto-
674 bacillus fermentum 104R That Binds to Porcine Small Intestinal Mucus and Gastric Mucin Purification and Charac-
675 terization of a Surface Protein from Lactobacillus fermentum 104R That Binds to ," 68(5). doi:
676 10.1128/AEM.68.5.2330.

677 Roos, S. *et al.* (1996) "A collagen binding protein from Lactobacillus reuteri is part of an ABC transporter system?,"
678 *FEMS Microbiology Letters*, 144(1). doi: 10.1016/0378-1097(96)00334-5.

679 Roos, S. and Jonsson, H. (2002) "A high-molecular-mass cell-surface protein from Lactobacillus reuteri 1063 ad-
680 heres to mucus components," *Microbiology*. England: Soc General Microbiol, 148(2). doi: 10.1099/00221287-148-2-
681 433.

682 Rosales-Mendoza, S., Angulo, C. and Meza, B. (2016) "Food-grade organisms as vaccine biofactories and oral de-
683 livery vehicles," *Trends in Biotechnology*. Elsevier Ltd, 34(2). doi: 10.1016/j.tibtech.2015.11.007.

Rud, I. *et al.* (2006) "A synthetic promoter library for constitutive gene expression in Lactobacillus plantarum," *Microbiology*, 152(4). doi: 10.1099/mic.0.28599-0.

Salas-Jara, M. *et al.* (2016) "Biofilm Forming Lactobacillus: New Challenges for the Development of Probiotics," *Microorganisms*, 4(4). doi: 10.3390/microorganisms4030035.

Saraiva, T. D. L. *et al.* (2015) "Milk fermented with a 15-lipoxygenase-1-producing Lactococcus lactis alleviates symptoms of colitis in a murine model.," *Current pharmaceutical biotechnology*, 16(5). doi: 10.2174/1389201015666141113123502.

Scaldaferri, F. *et al.* (2016) "Role and mechanisms of action of Escherichia coli Nissle 1917 in the maintenance of remission in ulcerative colitis patients: an update," *World Journal of Gastroenterology*, 22(24). doi: 10.3748/wjg.v22.i24.5505.

Shafaghi, A. *et al.* (2016) "The Effect of Probiotic Plus Prebiotic Supplementation on the Tolerance and Efficacy of Helicobacter Pylori Eradication Quadruple Therapy: a Randomized Prospective Double Blind Controlled Trial," *Middle East Journal of Digestive Diseases*. Iranian Society of Gastroenterology and Hepatology, 8(3). doi: 10.15171/mejdd.2016.30.

Shreiner, A. B., Kao, J. Y. and Young, V. B. (2015) "The Gut Microbiome in Health and in Disease," *Curr Opin Gastroenterol*. NIH Public Access, 31(1). doi: 10.1097/MOG.0000000000000139.The.

Tallon, R. *et al.* (2007) "Strain- and matrix-dependent adhesion of Lactobacillus plantarum is mediated by proteinaceous bacterial compounds," *Journal of Applied Microbiology*, 102(2). doi: 10.1111/j.1365-2672.2006.03086.x.

Troge, A. *et al.* (2012) "More than a marine propeller - the flagellum of the probiotic Escherichia coli strain Nissle 1917 is the major adhesin mediating binding to human mucus," *International Journal of Medical Microbiology*. Elsevier GmbH., 302(7–8), pp. 304–314. doi: 10.1016/j.ijmm.2012.09.004.

Uchida, H. *et al.* (2004) "A New Assay Using Surface Plasmon Resonance (SPR) to Determine Binding of the Lactobacillus acidophilus Group to Human Colonic Mucin," *Bioscience, Biotechnology, and Biochemistry*, 68(5). doi: 10.1271/bbb.68.1004.

US National Library of Medicine (2018) *Search: Probiotic; Lactic Acid Bacteria; Intestine | Exclude Unknown | Completed | 01/012018 - 12/31/2018*.

Valeriano, V. D. *et al.* (2016) "Carbohydrate-binding specificities of potential probiotic Lactobacillus strains in porcine jejunal (IPEC-J2) cells and porcine mucin," *Journal of Microbiology*, 54(7). doi: 10.1007/s12275-016-6168-7.

Wagner, C. E., Wheeler, K. M. and Ribbeck, K. (2018) "Mucins and Their Role in Shaping the Functions of Mucus Barriers," *Annual Review of Cell and Developmental Biology*, 34(1). doi: 10.1146/annurev-cellbio-100617-062818.

Waller, M. C. *et al.* (2017) "Toward a genetic tool development pipeline for host-associated bacteria," *Current Opinion in Microbiology*. Elsevier Ltd, 38, pp. 156–164. doi: 10.1016/j.mib.2017.05.006.

Walter, J., Britton, R. A. and Roos, S. (2011) "Host-microbial symbiosis in the vertebrate gastrointestinal tract and the Lactobacillus reuteri paradigm," *Proc Natl Acad Sci U S A*, 108 Suppl. doi: 10.1073/pnas.1000099107.

West, K. A. *et al.* (2019) " An engineered E. coli Nissle improves hyperammonemia and survival in mice and shows dose-dependent exposure in healthy humans ," *Science Translational Medicine*, 11(475). doi: 10.1126/scitranslmed.aau7975.

Wickström, C. *et al.* (2013) "Surface-associated MUC5B mucins promote protease activity in Lactobacillus fermentum biofilms," *BMC Oral Health*, 13(1). doi: 10.1186/1472-6831-13-43.

724 Zanin, M. *et al.* (2016) "The Interaction between Respiratory Pathogens and Mucus," *Cell Host and Microbe*. Elsevier
725 Inc., 19(2). doi: 10.1016/j.chom.2016.01.001.

726 Zhang, Yunlei *et al.* (2012) "Escherichia coli Nissle 1917 targets and restrains mouse b16 melanoma and 4T1 breast
727 tumors through expression of azurin protein," *Applied and Environmental Microbiology*, 78(21), pp. 7603–7610. doi:
728 10.1128/AEM.01390-12.

729

730